PAPER *Special Section on EUs FP7 ICT R and D Project Activities on Future Broadband Access Technologies*

Performance Analysis of Cooperative-ARQ Schemes in Free-Space Optical Communications

Vuong V. MAI[†], ***Student Member and*** **Anh T. PHAM**[†*], ***Member***

SUMMARY We theoretically analyze the performance of free-space optical (FSO) systems using cooperative-ARQ (C-ARQ), a joint scheme of automatic-repeat-request (ARQ) and cooperative diversity, over atmospheric turbulence channels. We also propose a modified C-ARQ (M-C-ARQ) scheme that allows relay nodes to store a copy of frames for the more efficient response to transmission failure so that both transmission delay and energy consumption can be improved. Using Markov chain-based analytical models for both schemes, the system performance is analytically studied in terms of frame-error rate, goodput and energy efficiency, which directly reflect the transmission delay and energy consumption. Numerical results confirm that the proposed schemes outperform conventional ones. In addition, we discuss cross-layer design strategies for selecting parameters in both physical and link layers in order to optimize the performance of FSO systems over different atmospheric turbulence conditions and channel distances.

key words: *FSO, Cooperative diversity, ARQ, Energy efficiency*

1. Introduction

Free-space optical communications (FSO) is a transmission technology based on the propagation of light in free space. Compared to conventional wireless technologies using radio frequency (RF) signal, FSO offers a number of important advantages including the availability of vast and license-free spectrum, which allows the flexible provision of much higher data rates [1]. One of major challenging issues in practical deployment of FSO systems, especially over extended links, is the atmospheric turbulence. Caused by variations of the air refractive-index due to solar heating and wind, atmospheric turbulence results in rapid fluctuations in both intensity and phase of received signals [2]. This leads to an increase in the link error probability, which degrades the reliability of FSO systems.

Significant research efforts have been devoted to enhance FSO system reliability in the presence of atmospheric turbulence [3]–[13], and they can be mainly classified into two groups: physical layer and link layer approaches. In the physical layer of FSO systems, many proposals have been reported, including fast multiple-symbol detection [3], maximum-likelihood sequence detection [4], multi-hop transmission [5], and cooperative diversity [6]–[9]. Among them, cooperative diversity has received an emerging interest due to its remarkable performance improvement by the introduction of additional degrees of freedom in the spatial dimension. The key operation of cooperative diversity systems is based on using multiple relay nodes between the source and the destination to create a virtual multiple-apertures, which is often referred to as parallel-relaying system.

On the other hand, automatic-repeat-request (ARQ), an efficient control mechanism for reliable transmissions at the link layer [10], has been recently considered for FSO communications [11]–[13]. The main concept of ARQ is that the destination requests the source to re-transmit a frame when it is incorrectly received. In [12], the frame-error rate of conventional ARQ and hybrid-ARQ (H-ARQ) protocols has been evaluated taking into account the case of weak-to-moderate turbulence conditions. In [13], Aghajanzadeh *et al*. provided insight into the outage probability of different H-ARQ protocols in the strong turbulence regimes and demonstrated that performance gains can be achieved through the deployment of H-ARQ. Note that despite providing a higher reliable transmission, both conventional ARQ and H-ARQ protocols suffer from high delay and high energy consumption due to re-transmission processes. These points, however, have not been addressed in previous studies of FSO systems.

It is important to emphasize that although employing either cooperative diversity or ARQ, in several conditions (i.e., high turbulence strengths or long-distance transmissions), FSO system reliability can be still degraded to unacceptable levels. Motivated by ideas in RF wireless communications, which have recently received increasing interests to deal with fading channels [14]–[16], we introduce, for the first time within the context of FSO communications, the joint design approach using ARQ and cooperative diversity, namely cooperative-ARQ (C-ARQ). Moreover, we propose a modified C-ARQ (M-C-ARQ) scheme to improve the system performance over turbulence channels. Using Markov chain-based analytical models, the system performance is analytically studied in terms of frame-error rate, goodput and energy efficiency, which directly reflect both the transmission delay and energy consumption. Numerical results confirm that the proposed schemes outperform conventional ones, and the newly proposed M-C-ARQ offers a significant performance improvement. We also discuss cross-layer design

[†]The author are with the Computer Communications Lab., The University of Aizu, Aizuwakamatsu, Fukushima, Japan 965-8580

[*]E-mail: pham@u-aizu.ac.jp

DOI: 10.1587/transcom.E94.B.1

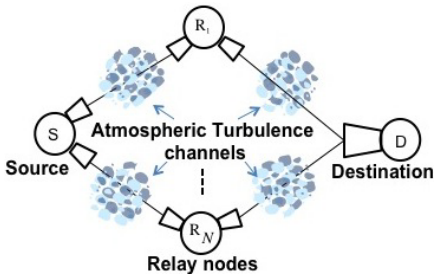

Fig. 1 System scenario.

strategies for selecting parameters of both physical and link layers to optimize the system performance in various contexts of atmospheric turbulence conditions and channel distances.

The remainder of the paper is organized as follows. The system description is presented in Section 2. In Section 3, unsuccessfully receiving frame probability, Markov chain parameters and performance parameters are derived. Numerical results are given in Section 4. Finally, Section 5 concludes the paper.

2. System Description

We consider a cooperative FSO system realized by a parallel-relaying structure as depicted in Fig. 1. The communication between the source (S) and the destination (D) is achieved through N relay nodes (R_i, $1 \le i \le N$) placed between S and D. S is equipped with N transmitters and each of them points out to the corresponding relay node. At D, a large field-of-view receiver is employed, which allows to simultaneously detect optical signals from all relay nodes. Throughout this paper, we assume that the sub-carrier binary phase-shift keying modulation (SC-BPSK) is employed. We also assume that shot noise caused by background radiation is the dominant noise source with respect to signal-dependent shot noise, thermal noise and dark current. As a result, noise at each receiver can be modeled as signal-independent additive white Gaussian noise (AWGN) with zero mean and variance σ_N^2.

2.1 Turbulence Channel Model

We examine the FSO channel between two terminals A and B. Considering both effects of channel loss (a_{AB}) and atmospheric turbulence (X_{AB}), the channel gain is defined as

$$H_{\mathrm{AB}} = a_{\mathrm{AB}} X_{\mathrm{AB}}. \tag{1}$$

The channel loss, due to molecular absorption and aerosol scattering suspended in the air, is given by [2]

$$a_{\mathrm{AB}} = \frac{r^2}{(\phi l_{\mathrm{AB}})^2} \exp(-\beta l_{\mathrm{AB}}), \tag{2}$$

where r, l_{AB}, ϕ and β are the receiver aperture diameter, the channel distance, the angle of divergence in radian and the atmospheric extinction coefficient, respectively.

2.1.1 Log-normal Turbulence Model

In case of weak-to-moderate turbulence, it is generally accepted that the influence of turbulence is modeled as a random process with log-normal distribution whose probability density function (pdf) is given as

$$f_{X_{\mathrm{AB}}}(x) = \frac{1}{\sqrt{2\pi}\sigma_s x} \exp\left[-\frac{\left(\ln x + \sigma_s^2/2\right)^2}{2\sigma_s^2}\right], \tag{3}$$

where σ_s^2 is the log intensity variance that depends on the channel characteristics as given by [17]

$$\sigma_s^2 = \exp\left[\frac{0.49\sigma_R^2}{\left(1+0.18d^2+0.56\sigma_R^{12/5}\right)^{7/6}} + \frac{0.51\sigma_R^2}{\left(1+0.9d^2+0.62d^2\sigma_R^{12/5}\right)^{5/6}}\right] - 1. \tag{4}$$

Here, $d = \sqrt{kD^2/4l_{\mathrm{AB}}}$, where $k = 2\pi/\lambda$ is the optical wave number, and D is the receiver aperture diameter. σ_R^2 is the Rytov variance, and in case of plane wave propagation, it is given by

$$\sigma_R^2 = 1.23 C_n^2 k^{7/6} l_{\mathrm{AB}}^{11/6}, \tag{5}$$

where C_n^2 is the turbulence strength, which typically varies from $10^{-17}\mathrm{m}^{-2/3}$ to $10^{-13}\mathrm{m}^{-2/3}$.

2.1.2 Gamma-Gamma Turbulence Model

In strong atmospheric turbulence conditions ($C_n^2 > 5\times10^{-15}\mathrm{m}^{-2/3}$), it is generally accepted that the atmospheric turbulence is modeled as a random process X_{AB} with Gamma-Gamma distribution [19]. Its corresponding pdf is given by

$$f_{X_{\mathrm{AB}}}(x) = \frac{2(\alpha_{\mathrm{AB}}\beta_{\mathrm{AB}})^{(\alpha_{\mathrm{AB}}+\beta_{\mathrm{AB}})/2}}{\Gamma(\alpha_{\mathrm{AB}})\Gamma(\beta_{\mathrm{AB}})} x^{(\alpha_{\mathrm{AB}}+\beta_{\mathrm{AB}})/2-1} \times K_{\alpha_{\mathrm{AB}}-\beta_{\mathrm{AB}}}\left(2\sqrt{\alpha_{\mathrm{AB}}\beta_{\mathrm{AB}}x}\right), \tag{6}$$

where $\Gamma(.)$ is the gamma function, and $K_{\alpha_{\mathrm{AB}}-\beta_{\mathrm{AB}}}(.)$ is the modified Bessel function of the second kind and order $\alpha_{\mathrm{AB}}-\beta_{\mathrm{AB}}$. α_{AB} and β_{AB} are the pdf parameters, which are expressed as functions of Rytov variance σ_R^2 [20]:

$$\alpha_{\mathrm{AB}} = \left\{\exp\left[\frac{0.49\sigma_R^2}{\left(1+1.11\sigma_R^{12/5}\right)^{7/6}}\right] - 1\right\}^{-1},$$

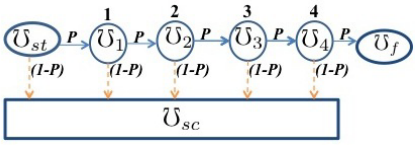

Fig. 2 Markov chain model for C-ARQ when $M = 4$.

$$\beta_{\mathrm{AB}} = \left\{ \exp\left[\frac{0.51\sigma_R^2}{\left(1 + 0.69\sigma_R^{12/5}\right)^{5/6}} \right] - 1 \right\}^{-1}. \quad (7)$$

Here, σ_R is defined as in Eq. (5).

We assume that all relay nodes are placed in the middle between S and D, i.e. the channel distance for S-R$_i$ and R$_i$-D links are equal ($l_{\mathrm{SR}_i} = l_{\mathrm{R}_i\mathrm{D}} \approx 1/2 l_{\mathrm{SD}}$). Therefore, the channel gain of each link in the system can be calculated with the same values of channel loss (denoted as a) and parameters of turbulence models. This assumption is generally acceptable in studies of parallel-relaying systems [9].

2.2 Proposed Cooperative-ARQ Schemes

2.2.1 C-ARQ Scheme

The C-ARQ scheme works as follows. Initially, the source node broadcasts a frame to all relay nodes. A relay node, which successfully receives the frame, is called as a successful relay node and denoted as R$^{\mathrm{s}}$. All R$^{\mathrm{s}}$s then forward the frame to the destination and also send back acknowledge (ACK^R) messages to S to notify their successes of receiving the frame. The connections between R$^{\mathrm{s}}$s and D actually form a MISO (Multiple Inputs, Single Output) link. At the D side, if the frame is successfully received over the MISO link, D sends back an ACK^D message to S through relay nodes, otherwise a negative acknowledge (NACK) message is sent. For the sake of simplicity, it is assumed that reverse connections from D back to S are error-free. We denote the duration from the instant that S broadcasts the frame to the instant that all feedback messages come back to S as a transmission round. After the initial transmission round, based on feedback messages, S has the knowledge of either a success or a failure of frame delivery. The failure happens when either no ACK^R is received (no relay node successfully receives the frame from S) or a NACK is received (D does not successfully receive the frame from MISO link). On the contrary, an ACK^D notifies D the successful transmission.

When a successful transmission occurs, S moves on to transmit a new frame. Meanwhile, in the failed transmission case, S re-transmits the recent frame. After the maximum number of re-transmission rounds, M (i.e., the persistent level), if D still cannot successfully receive the frame, S stops re-transmitting and gives up.

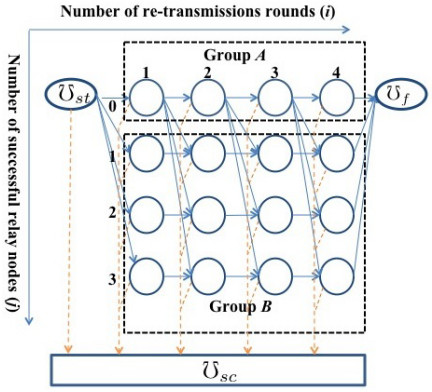

Fig. 3 Markov chain model for M-C-ARQ when $M = 4$ and $N = 3$.

The behavior of C-ARQ can be modeled as a Markov chain, as shown in Fig. 2. In this figure, the C-ARQ operation can be separated into four state groups: $\mho_{st}$ state: the S begins the initial transmission round; $\mho_i$ state (circle symbols): C-ARQ is in the i-th re-transmission round ($1 \le i \le M$); $\mho_{sc}$ state: the recovery process is successful; $\mho_f$ state: the recovery process is failed.

2.2.2 M-C-ARQ Scheme

In the C-ARQ scheme, as relay nodes only play a role of forwarding the frame to the destination, the source has to re-broadcast the frame to all relay nodes when re-transmissions are needed. This action results in additional delay and energy consumption. To improve the system performance, in the M-C-ARQ scheme, relay nodes are designed with a function of storing a copy of frame. In particular, each successful relay node in the initial transmission round stores a copy of the frame before forwarding it to D. After this transmission round, in the case of failed transmission, there are two strategies for re-transmitting the frame corresponding to two kinds of failure. Firstly, If no ACK^R is received, S re-broadcasts the frame to all relay nodes due to the fact that no relay node successfully received the frame in the previous transmission round. Secondly, if a NACK arrives, S knows that there are some R$^{\mathrm{s}}$s and they are keeping copies of frame. Therefore, S keeps silent and waits; wheres using the copies, R$^{\mathrm{s}}$s re-transmit the frame to D. To this end, the re-broadcast of frame from the source to all relay nodes are no longer needed, and thus M-C-ARQ is expected to reduce delay and energy consumption. After M attempts of transmission rounds, and D does not receive successfully the frame, M-C-ARQ gives up the recovery process.

Figure 3 illustrates the Markov chain model for the operation of M-C-ARQ scheme when $M = 4$ and $N = 3$. While definitions of $\mho_{st}$, $\mho_{sc}$ and $\mho_f$ are the same as ones used in C-ARQ, each element of re-

transmission rounds is defined by $\mho_{(i,j)}$, where i, j represents the number of re-transmission rounds and the number of R$^{\text{s}}$s, respectively. $\mho_{(i,j)}$ is also classified into two groups:

$A = \{\mho_{(i,0)} \mid 1 \le i \le M\}$: M-C-ARQ is in the i-th re-transmission round and S re-broadcasts the frame to all relay nodes in order to start this round.

$B = \{\mho_{(i,j)} \mid 1 \le i \le M, 1 \le j \le N\}$: M-C-ARQ is in the i-th re-transmission round and this round is created by using the copies of frame from j R$^{\text{s}}$s.

3. Performance Analysis

In this section, Markov chain models are employed to analytically analyze the system performance. Because after a re-transmission round, the events of unsuccessfully receiving the frame at relay nodes or D result in transiting states in Markov chains, it is important to derive probabilities of such events first.

3.1 Unsuccessfully Receiving Frame Probability

We assume that all frames have a length of L bits and the error correction (FEC) algorithm, which can correct up to t bit-errors, is employed by the physical layer. The probability of unsuccessfully receiving the frame in D is defined as the probability that there are more than t bit-errors in a frame. It therefore can be expressed as

$$P_D(j) = 1 - \sum_{k=0}^{t} \binom{L}{k} P_b(j)^k [1 - P_b(j)]^{L-k}, \quad (8)$$

where $P_b(j)$ is the bit-error rate at MISO link.

In order to calculate $P_b(j)$, we denote $\mathbb{S}$ as the successful set, which is the set of j R$^{\text{s}}$s. The output signal of photodetector in this case can be obtained by

$$r_D = m\bar{g}\Re s(t) \sum_{i \in \mathbb{S}} a_{\text{R}_i\text{D}} X_{\text{R}_i\text{D}} + n_D(t), \quad (9)$$

where $s(t)$ is the transmitted signal, m is the modulation index, $\bar{g}$ is the average receiver gain, $\Re$ is the photodetector responsivity, and $n_D(t)$ is the signal-independent AWGN at the receiver with zero mean and variance σ_N^2. $a_{\text{R}_i\text{D}}$ and $X_{\text{R}_i\text{D}}$ express effects of channel loss and atmospheric turbulence in the link from i-th relay node to D, respectively.

When the turbulence is modeled by log-normal channel, referring to Section 2.1.1, we have $a_{\text{R}_i} = a$ and $I = \sum_{i \in \mathbb{S}} X_{\text{R}_i\text{D}}$ is a sum of j independent and identically distributed log-normal random variables (L-N RVs). According to the well known Feton-Wilkilson's method [18], I can be closely approximated by a L-N RVs whose pdf is expressed as follows

$$f_I(y) = \frac{1}{\sqrt{2\pi}\sigma_{s,I} y} \exp\left[-\frac{(\ln y + \sigma_{s,I}^2/2)^2}{2\sigma_{s,I}^2} \right], \quad (10)$$

where

$$\sigma_{s,I}^2 = \ln\left[1 + (\exp(\sigma_s^2) - 1)/j\right]. \quad (11)$$

In FSO systems employing SC-BPSK, $P_b(j)$ is given as [19]

$$P_b(j) = \int_0^\infty Q\left(y\sqrt{\text{SNR}}\right) f_I(y) dy, \quad (12)$$

where $Q(z) = \frac{1}{\sqrt{2\pi}} \int_z^\infty \exp(-\frac{z^2}{2}) dz$ is the Gaussian Q-function and SNR is signal-to-noise ratio.

$$\text{SNR} = (\frac{m\bar{g}\Re P_s a}{4\sigma_N})^2, \quad (13)$$

with P_s is the transmitted power per transmitter.

Making the change of variable $\hbar = \frac{(\ln y + \sigma_{s,I}^2/2)}{\sqrt{2}\sigma_{s,I}}$ we have

$$P_b(j) = \frac{1}{\sqrt{\pi}} \int_{-\infty}^{\infty} Q\left[\sqrt{\text{SNR}} \exp(\sqrt{2}\sigma_{s,I}\hbar - \sigma_{s,I}^2/2)\right] \times \exp(-\hbar^2) d\hbar. \quad (14)$$

Using the approximation

$$\int_{-\infty}^{\infty} g(\hbar) \exp(-\hbar^2) d\hbar \approx \sum_{i=-N; i\neq 0}^{N} w_i g(\hbar_i), \quad (15)$$

where w_i and $\hbar_i$, in which $i = (-N, -N+1, ..., N)$, are the weight factors and the zeros of Hermite polynomial, respectively, we can obtain a tractable expression of $P_b(j)$, that is

$$P_b(j) \approx \frac{1}{\sqrt{\pi}} \sum_{i=-N; i\neq 0}^{N} w_i \times Q\left[\sqrt{\text{SNR}} \exp(\sqrt{2}\sigma_{s,I}\hbar_i - \sigma_{s,I}^2/2)\right]. \quad (16)$$

For Gamma-Gamma channels, according to the study in [21], the sum of j independent and identically distributed Gamma-Gamma random variables (G-G RVs), $\sum_{i \in \mathbb{S}} X_{\text{R}_i\text{D}}$, can be closely approximated by another G-G RV denoted as I. Note that, $\alpha_{\text{R}_i\text{D}} = \alpha_{\text{R}_k\text{D}} = \alpha$ and $\beta_{\text{R}_i\text{D}} = \beta_{\text{R}_k\text{D}} = \beta, \forall \{i, k\} \subset \mathbb{S}$ are assumed, and the pdf of I is obtained as follows

$$f_I(y) = \frac{2(\alpha_I\beta_I/j)^{(\alpha_I+\beta_I)/2}}{\Gamma(\alpha_I)\Gamma(\beta_I)} y^{(\alpha_I+\beta_I)/2-1} \times K_{\alpha_I-\beta_I}\left(2\sqrt{\alpha_I\beta_I x/j}\right), \quad (17)$$

with the parameters

$$\beta_I = \frac{(1+e) + \sqrt{(1+e)^2 + \frac{4}{j\alpha^2}k_1}}{2(e + \frac{1}{\alpha} + 1)} \beta j, \alpha_I = \frac{\beta_I}{e},$$
$$k_1 = (\alpha + \beta + 1), e = \frac{\beta}{\alpha}. \quad (18)$$

Based on a series expansion for modified Bessel function, we obtain the closed-form of $P_b(j)$ as follows

$$\begin{aligned} P_b(j) &= \int_0^\infty Q\left(y\sqrt{\mathrm{SNR}}\right) f_I(y)dy \\ &= A(\alpha_I,\beta_I)j^{-\frac{\alpha_I+\beta_I}{2}} \sum_{p=0}^{\infty} j^{-\frac{2p-\alpha_I+\beta_I}{2}} \\ &\times [a_p(\alpha_I,\beta_I)B(\frac{1}{2},\frac{p+\beta_I+1}{2})(\frac{\mathrm{SNR}}{2})^{-\frac{p+\beta_I}{2}} \\ &- a_p(\beta_I,\alpha_I)B(\frac{1}{2},\frac{p+\alpha_I+1}{2})(\frac{\mathrm{SNR}}{2})^{-\frac{p+\alpha_I}{2}}], \end{aligned} \tag{19}$$

where the form of $A(\alpha_I,\beta_I), a_p(x,y)$ and $B(x,y)$ can be found in [22] [Eqs. (7)–(8)].

Finally, the derivation of $P_D(j)$ can be used for calculating the failure of frame delivery in a link from S to a relay node (P_{re}). Due to the fact that both S-R and R-D links are employed with the same parameters of channel gain (as mentioned in Section 2), we have: $P_{re} = P_D(j)$ with $j = 1$, which corresponds to the case of only one R$^{\mathrm{s}}$ forwarding the frame to D.

3.2 Markov Chain Parameters

3.2.1 State-Transition Probabilities

Based on state definitions in Section 2.2, we get state transition probabilities for the Markov chain models, which are functions of $P_D(j)$ and P_{re}. For C-ARQ, in the horizontal direction of Fig. 2, all transition probabilities are equal (P). It is the probability of unsuccessfully transmitting the frame in a transmission round, which happens when either no relay node successfully receives the frame from S or D does not successfully receive the frame in MISO link. In the vertical direction, transition probabilities express the probability of successfully transmitting the frame and are given as $(1-P)$.

$$P = P_{re}^N + \sum_{j=1}^{N} \binom{N}{j} (1-P_{re})^j P_{re}^{N-j} P_D(j). \tag{20}$$

For M-C-ARQ, we first consider a state belonging to $\mho_{st}$ or group A. In this state, since the transmission round is started by re-broadcasting the frame to all relay nodes, three cases may happen: 1) the transmission round is success, 2) there is no R$^{\mathrm{s}}$ and 3) there are j R$^{\mathrm{s}}$s but D does not received successfully the frame. State transition probabilities related to those cases are expressed in turn as follows

$$\begin{aligned} P_{\mho_{st}\to\mho_{sc}} &= P_{\mho_{(i,0)}\to\mho_{sc}} = 1-P; \\ P_{\mho_{st}\to\mho_{(i,0)}} &= P_{\mho_{(i,0)}\to\mho_{(i,0+1)}} = P_{\mho_{(M,0)}\to\mho_f} = P_{re}^N; \\ P_{\mho_{st}\to\mho_{(1,j)}} &= P_{\mho_{(i,0)}\to\mho_{(i+1,j)}} = \\ &= \binom{N}{j} (1-P_{re})^j P_{re}^{N-j} P_D(j), j \neq 0. \end{aligned} \tag{21}$$

In group B, a state $\mho_{(i,j)}$ goes to $\mho_{sc}$ state with a probability of $1-P_D(j)$ or goes to another state with a probability of $P_D(j)$. They correspond to the success or failure of transmission created by j R$^{\mathrm{s}}$s.

3.2.2 State Probabilities

In Markov chain models, since a given frame transmission is always started as the $\mho_{st}$ state, the state probability of $\mho_{st}$ is set as 1. By using the initial state probability ($P(\mho_{st}) = 1$) and state transition probabilities, we can obtain all state probabilities. For example, probabilities of state of the first column in Fig. 3 can be calculated as:

$$P(\mho_{(0,j)}) = P(\mho_{st}) P_{\mho_{st}\to\mho_{(0,j)}}. \tag{22}$$

In other columns, state probabilities can be obtained by using state probabilities of the previous column and corresponding state transition probabilities. For instance, state probabilities of group A and group B are expressed in turn as follows

$$\begin{aligned} P(\mho_{(i,0)}) &= P(\mho_{(i-1,0)}) P_{\mho_{(i-1,0)}\to\mho_{(i,0)}}, i \neq 1; \\ P(\mho_{(i,j)}) &= P(\mho_{(i-1,0)}) P_{\mho_{(i-1,0)}\to\mho_{(i,j)}} \\ &\quad + P(\mho_{(i-1,j)}) P_{\mho_{(i-1,j)}\to\mho_{(i,j)}}, i \neq 1, j \neq 0. \end{aligned} \tag{23}$$

Similarly, we obtain state probabilities in retransmission rounds of C-ARQ:

$$P(\mho_i) = P(\mho_{(i-1)}) P, i \neq 1. \tag{24}$$

3.3 Performance Metrics

3.3.1 Frame-Error Rate

We define frame-error rate, FER, as the probability that the recovery process is failed. Obviously, it is $\mho_f$ state probability and given as

$$\begin{aligned} \mathrm{FER}_{\text{C-ARQ}} &= P(\mho_M) P_{\mho_M\to\mho_f}; \\ \mathrm{FER}_{\text{M-C-ARQ}} &= \sum_{j=0}^{N} P(\mho_{(M,j)}) P_{\mho_{(M,j)}\to\mho_f}. \end{aligned} \tag{25}$$

3.3.2 Goodput

Goodput, $\mathbb{G}$, is defined as the ratio of the number of successfully received data unit (bits) and the average total delay ($\mathbb{D}$) required to successfully deliver a frame. Goodput is therefore given as $\mathbb{G} = L(1-\mathrm{FER})/\mathbb{D}$.

We denote T as the total time required for normally transmitting a frame through a single link (total

time consumption for frame transmission, error detection, and so on in either a S-R$_i$ or R$_i$-D link). As seen in Eq. (26), for C-ARQ, $\mathbb{D}_{\text{C-ARQ}}$ consists of two parts: the first part expresses the time for initial transmission round, while the second one is for counting the time consumption in re-transmission rounds. In the equation for $\mathbb{D}_{\text{M-C-ARQ}}$, the part related to the time consuming in re-transmission rounds is divided into two sub-parts, which correspond to states in group A and B. It is worth noting that in group B, because re-transmission round is created by R$^{\text{s}}$s, the time consumption per round is only one T.

$$\begin{aligned}\mathbb{D}_{\text{C-ARQ}} &= 2T + 2T\sum_{i=1}^{M} iP(\mho_i);\\ \mathbb{D}_{\text{M-C-ARQ}} &= 2T + 2T\sum_{i=1}^{M} iP(\mho_{(i,0)})\\ &\quad + T\sum_{j=1}^{N}\sum_{i=1}^{M} iP(\mho_{(i,j)}).\end{aligned} \tag{26}$$

3.3.3 Energy Efficiency

Energy efficiency, $\Im$, is defined as the ratio of the number of successfully received data units (bits) and the total energy (E) consumed by all transmitters in successfully delivering a frame. It is therefore given as $\Im = L(1 - \text{FER})/E$. Similarly, the total energy consumptions for C-ARQ and M-C-ARQ schemes can be expressed as

$$\begin{aligned}E_{\text{C-ARQ}} &= \mathbb{E} + \mathbb{E}\sum_{i=1}^{M} iP(\mho_i);\\ E_{\text{M-C-ARQ}} &= \mathbb{E} + \mathbb{E}\sum_{i=1}^{M} iP(\mho_{(i,0)})\\ &\quad + \mathbb{E}_f\sum_{j=1}^{N}\sum_{i=1}^{M} jiP(\mho_{(i,j)}).\end{aligned} \tag{27}$$

In above equations, $\mathbb{E} = \mathbb{E}_f(N + \sum_{j=1}^{N} jP(\mho_{(0,j)}))$ is the average energy consumption for the initial transmission round, $\mathbb{E}_f = L\frac{P_s}{2}$ is the frame energy ($\frac{P_s}{2}$ is a half of the peak transmitted power used to express a bit energy for SC-BPSK modulation). The appearance of factor j in the multiplication is for indicating the number of R$^{\text{s}}$s that contribute energy to the frame delivery.

4. Numerical Results and Discussions

In this section, using previously derived equations, we numerically analyze the system performance for three cases: 1) using a parallel-relaying system without ARQ, 2) using the C-ARQ scheme, and 3) using the M-C-ARQ scheme. Note that, the first one is a special case of using C-ARQ when $M = 0$. Throughout the analysis, for a fair comparison, the total transmitted power constraint is assumed. It is also assumed that the total transmitted power is to be equally allocated to all transmitters, i.e., the relationship between the total transmitted power (P_t) and the transmitted power per transmitter (P_s, as mentioned in Eq. (13)) is given by: $P_t = 2NP_s$, where $(2N)$ expresses total number of transmitters in the whole system. Table 1 shows the system parameters and constants used in the numerical analysis.

Table 1 System Parameters and Constants

Name	Symbol	Value
Frame size	L	128 bits
FEC parameter	t	1
Frame transmission time in single link	T	10 ms
Modulation index	m	1
Receiver noise variance	σ_N^2	1.5×10^{-13}
Average receiver gain	$\overline{g}$	15
Responsivity	$\Re$	1 A/W
Receiver aperture diameter	r	0.02 m
Atmospheric extinction coefficient	β	0.1 dB/km
Angle of divergence	ϕ	10^{-3} radian
Wavelength	λ	1550 nm

4.1 Frame-Error Rate

First, in Figs. 4 and 5, we highlight the advantage of proposed schemes in the improvement of the frame-error rate by comparing the performance of the system in cases of with and without ARQ. More specifically, Fig. 4 shows FER versus the total transmitted power for the different cases when $l_{\text{SD}} = 3,000$ m and $C_n^2 = 10^{-15}$ m$^{-2/3}$; the required total transmitted power to achieve a specific value of FER (10^{-8}) versus the persistence level when N =2, $l_{\text{SD}} = 3,000$ m, and $C_n^2 = 10^{-15}$ m$^{-2/3}$ is shown in Fig. 5.

It is seen in the both figures that when either C-ARQ or M-C-ARQ is employed, lower P_t is required to achieve the same value of FER. For example, when $N = 2$ and $M = 2$ are employed, FER $= 10^{-8}$ in the system with C-ARQ can be achieved even when $P_t = -10.2$ dBm, whereas the system without ARQ requires $P_t = -9.5$ dBm to reach that FER. Moreover, compared to C-ARQ, M-C-ARQ has better performance. It is interesting that although the original idea, storing before forwarding the frame at relay nodes, is only expected to reduce time and energy consumption, the system performance in terms of frame-error rate gains additional benefits by using it. This is due to the fact that the probability of successfully transmitting the frame in a short transmission (from R$^{\text{s}}$ to

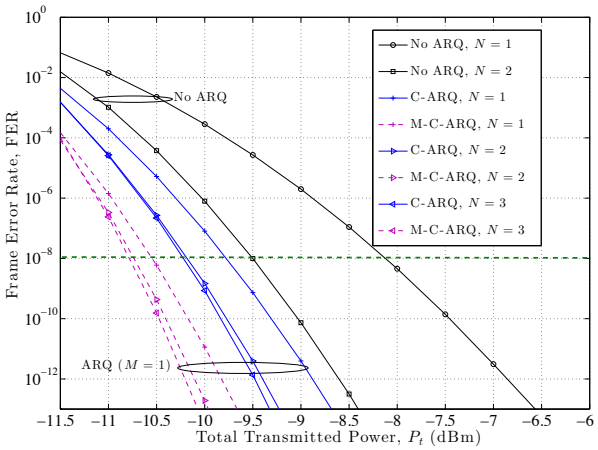

Fig. 4 Frame-error rate versus the total transmitted power when $C_n^2 = 10^{-15}\text{m}^{-2/3}$ and $l_{\text{SD}} = 3,000$ m.

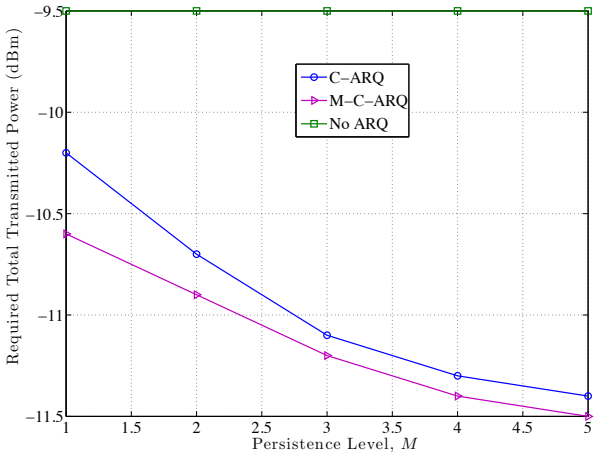

Fig. 5 Required total transmitted power to achieve FER=10^{-8} versus the persistence level (M) when $C_n^2 = 10^{-15}\text{m}^{-2/3}$, $N = 2$ and $l_{\text{SD}} = 3,000$ m.

D) is higher than that in a long transmission (from S to R^s and then from R^s to D).

In addition, there are other crucial points. Firstly, in Fig. 4, considering the parallel-relaying structure, the increase of N further improves the system performance. However, not much improvement can be seen when N becomes higher than 2. We therefore use $N = 2$ in the remaining discussion. Secondly, in Fig. 5, when increasing the value of the persistence level, the required total transmitted power decreases, thus by controlling M, the system could gain more benefits from ARQ schemes. This point will be discussed further in the next section.

4.2 Goodput

In Fig. 6, we analyze goodput of each scheme for various values of M. The limitation of C-ARQ is expressed by its lower goodput in comparison with the case of no ARQ. This is because of the high delay caused by re-transmission processes. Meanwhile, M-C-ARQ has the best performance in all cases due to its saving time strategy. More importantly, the increase of M also further improves goodput. However, there is no more improvement when M becomes higher than 4. This can be explained by two reasons: 1) an increase in persistence level decreases FER, yet increases the time consumption, especially in low power regime, and 2) FER improvement is saturated when M is high enough. These point are confirmed in Fig. 7, where the average total delay ($\mathbb{D}_{\text{M-C-ARQ}}$ in Eq. (26)) and frame-error rate ($\text{FER}_{\text{M-C-ARQ}}$) are analyzed for different values of M. It is therefore recommended to use $M = 4$ as the optimized value for analyzed systems.

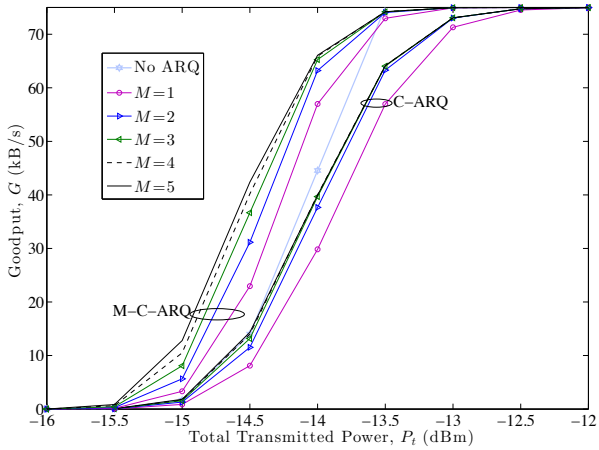

Fig. 6 Goodput versus the total transmitted power when N =2, $C_n^2 = 10^{-15}\text{m}^{-2/3}$ and $l_{\text{SD}} = 3,000$ m.

Next, Figs. 8 and 9 show goodput versus the total transmitted power with different channel distances for the weak and strong turbulence regimes, respectively. The turbulence strength is selected as follows: $C_n^2 = 10^{-15}\text{m}^{-2/3}$ for weak turbulence, $C_n^2 = 10^{-14}\text{m}^{-2/3}$ for strong turbulence. Channel distances of 3,000 and 4,000 m are considered. Using these figures, the impact of ARQ schemes, turbulence strength, channel distance, and total transmitted power on goodput can be comprehensively analyzed.

As is evident, an increase of turbulence strength results in an increase of required total transmitted power to achieve the same goodput. For example, in the case of no ARQ and $l_{\text{SD}} = 3,000$ m, in order to obtain the maximum goodput ($\mathbb{G}_{max} = 75$ kB/s), the required P_t are -11.2 dBm and -8.2 dBm for weak and strong turbulences, respectively. In addition, the system performance also depends strongly on the channel distance. More specifically, for the system with M-C-ARQ and considering the weak turbulence, an increase of l_{SD} by

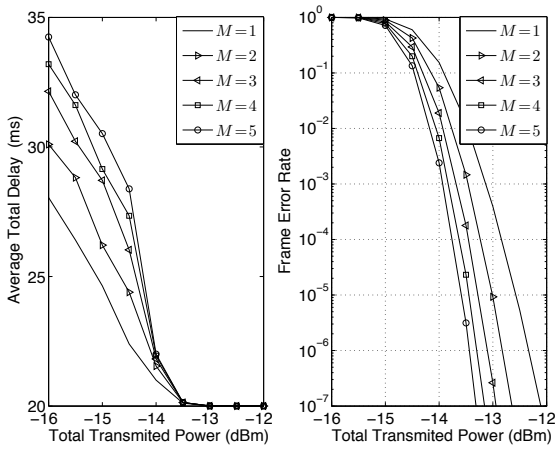

Fig. 7 Average total delay and frame-error rate versus the total transmitted power for different values of M when N =2, $C_n^2 = 10^{-15}\mathrm{m}^{-2/3}$, $l_{\mathrm{SD}} = 3,000$ m and employing M-C-ARQ.

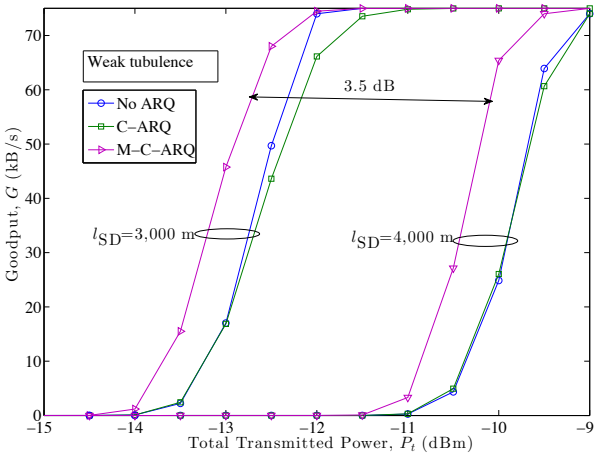

Fig. 8 Goodput versus the total transmitted power for different values of l_{SD} when N =2, $M = 4$ and $C_n^2 = 10^{-15}\mathrm{m}^{-2/3}$.

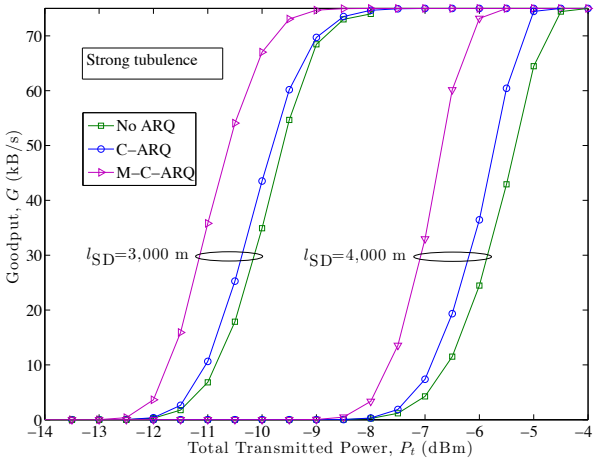

Fig. 9 Goodput versus the total transmitted power for different values of l_{SD} when N =2, $M = 4$ and $C_n^2 = 10^{-14}\mathrm{m}^{-2/3}$.

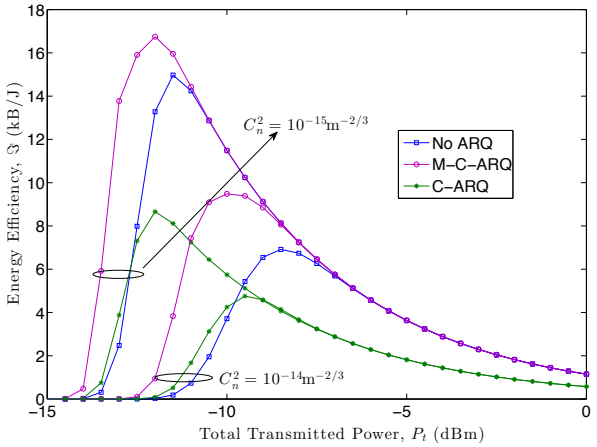

Fig. 10 Energy efficiency versus the total transmitted power when N =2, $M = 4$ and $l_{\mathrm{SD}} = 3,000$ m.

1,000 m leads to an increase of required peak transmitted power by approximately 3.5 dB to achieve the same value of $\mathbb{G}$.

These figures also confirm an important point that the benefit of ARQ schemes can be seen more clearly in worse conditions. Meanwhile, in the weak turbulence condition, the system without ARQ has better performance than the system employing C-ARQ, this phenomenon is reversed in the strong turbulence condition. Besides, in all conditions, M-C-ARQ has always the best performance.

4.3 Energy Efficiency

In Fig. 10, we analyze energy efficiency when $l_{\mathrm{SD}} = 3,000$ m, $M = 4$ and $N = 2$. Different ARQ schemes and values of the turbulence strength are considered. It is clear that there exists an optimal value of total transmitted power, P_{op}, at which energy efficiency is maximized. The presence of P_{op} is due to the fact that when the total transmitted power becomes high enough, the FER saturates, and any further increase of P_t only results in additional energy consumption. By considering P_{op} and maximum energy efficiency, $\Im_m$, in the following discussions, we further emphasize the advantage of M-C-ARQ.

In the case of weak turbulence, it is clear that M-C-ARQ is the best scheme in terms of using efficiently energy. For instance, the maximum energy efficiency are 17 kB/J, 15 kB/J and 8.5 kB/J for M-C-ARQ, no ARQ and C-ARQ, respectively. Nevertheless, the value of P_{op} seems like the same for all mentioned cases (−13.5 dBm). In the strong turbulence condition, the advan-

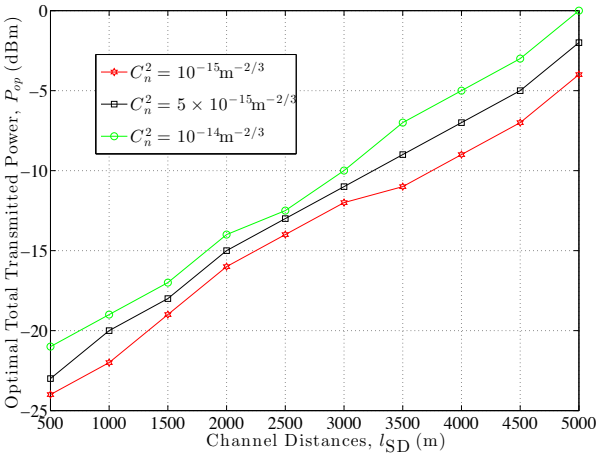

Fig. 11 Optimal total transmitted power versus the channel distance (l_{SD}) for difference values of C_n^2 when N =2, M = 4 and employing M-C-ARQ.

tage of M-C-ARQ can be seen more clearly. While $\Im_m$ of M-C-ARQ scheme is still higher than values of others, its P_{op} is the smallest one. More specifically, P_{op} is selected as −10 dBm, −9 dBm and −7 dBm for M-C-ARQ, C-ARQ and No ARQ, respectively.

Finally, the effects of both turbulence strengths and channel distances on energy efficiency, which employs M-C-ARQ scheme, are shown in Fig. 11. Using this figure, we can find the optimal total transmitted power for a specific turbulence strength and channel distance. Obviously, to achieve the maximum energy efficiency, the optimal total transmitted power should be increased when the channel distance increases. A higher turbulence strength requires a higher value of P_{op}. This figure allows us to select the range of optimal total transmitted power for a given channel distance. For example, when the channel distance is 4, 000 m, the range of P_{op} is from −9 to −5 dBm.

5. Conclusions

We have introduced C-ARQ for FSO communications to enhance the system reliability in the presence of atmospheric turbulences. We also proposed M-C-ARQ scheme to further improve system performances. Markov chain models were used to derive the system's frame-error rate, goodput and energy efficiency. Various physical and link layer parameters, including turbulence strength, total transmitted power, number of relay nodes, channel distances, and persistence level, were taken into account in the system performance analysis. The benefits of M-C-ARQ in enhancing FSO system reliability as well as reducing delay and energy were quantified. It was also shown that $M = 4$ and $N = 2$ are recommended values for the analyzed system. In addition, the optimal total transmitted power was investigated by considering the energy efficiency in different values of turbulence strength and channel distance.

References

[1] Z. Ghassemlooy, W.O. Popoola, and S. Rajbhandari, "Optical Wireless Communications System and Channel Modeling with Matlab," CRC publisher, USA, Aug. 2012.

[2] Z. Xiaoming, and J.M. Kahn, "Free-space optical communication through atmospheric turbulence channels," IEEE Trans. Commun., vol.50, no.8, pp.1293–1300, Aug. 2002.

[3] M.L.B. Riediger, R. Schober, and L. Lampe, "Fast multiple-symbol detection for free-space optical communications," IEEE Trans. Commun., vol.57, no.4, pp.1119–1128, Apr. 2009.

[4] N.D. Chatzidiamantis, G.K. Karagiannidis, and M. Uysal, "Generalized Maximum-Likelihood Sequence Detection for Photon-Counting Free Space Optical Systems," IEEE Trans. Commun., vol.58, no.12, pp.3381–3385, Dec. 2010.

[5] M. Safari, M.M. Rad, and M. Uysal, "Multi-Hop Relaying over the Atmospheric Poisson Channel: Outage Analysis and Optimization," IEEE Trans. Commun., vol.60, no.3, pp.817–829, Mar. 2012.

[6] C.A. Rjeily, and S. Haddad, "Cooperative FSO Systems: Performance Analysis and Optimal Power Allocation," IEEE/OSA J. Lightw. Techno., vol.29, no.7, pp.1058–1065, Apr. 2011.

[7] C. A. Rjeily, and A. Slim, "Cooperative diversity for free-space optical communications: transceiver design and performance analysis," IEEE Trans. Commun., vol. 53, pp. 658–663, Mar. 2011.

[8] C.A. Rjeily, "Performance Analysis of Selective Relaying in Cooperative Free-Space Optical Systems," IEEE/OSA J. Lightw. Techno., vol.31, no.18, pp.2965–2973, Sep. 2013.

[9] N.D. Chatzidiamantis, D.S. Michalopoulos, E.E. Kriezis, G.K. Karagiannidis, and R. Schober, "Relay selection protocols for relay-assisted free-space optical systems," , IEEE/OSA J. Opt. Commun. Netw., vol.5, no.1, pp.92–103, Jan. 2013.

[10] Y. Abdallah, M.A. Latif, M. Youssef, M., A. Sultan, and H. El-Gamal, "Keys Through ARQ: Theory and Practice," IEEE Trans. Infor. Forens. Security, vol.6, no.3, pp.737–751, Sep. 2011.

[11] C. Kose, and T.R. Halford, "Incremental redundancy hybrid ARQ protocol design for FSO links," Proc. IEEE Mil. Commun., pp.1–7, Boston, MA, Oct. 2009.

[12] K. Kiasaleh, "Hybrid ARQ for FSO Communications Through Turbulent Atmosphere," IEEE Commun. Lett., vol.14, no.9, pp.866–868, Sept. 2010.

[13] S.M. Aghajanzadeh, and M. Uysal, "Information Theoretic Analysis of Hybrid-ARQ Protocols in Coherent Free-Space Optical Systems," IEEE Trans. Commun., vol.60, no.5, pp.1432–1442, May 2012.

[14] L. Sangkook, W. Su, D.A. Pados, and J.D. Matyjas, "The Optimal Power Assignment for Cooperative Hybrid-ARQ Relaying Protocol," Proc. GLOBECOM 2011, pp.1–6, Houston, TX, USA, Dec. 2011.

[15] N. Marchenko, and C. Bettstetter, "Cooperative ARQ with Relay Selection: An Analytical Framework Using Semi-Markov Processes," IEEE Trans. Vehicular Techno., vol.63, no.1, pp.178–190, Jan. 2014.

[16] J. Ramis, and G. Femenias, "Cross-Layer QoS-Constrained Optimization of Adaptive Multi-Rate Wireless Systems using Infrastructure-Based Cooperative ARQ," IEEE Trans. Wireless Commun., vol.12, no.5, pp.2424–2435, May 2013.

[17] A.K. Majumdar, "Free-space laser communication performance in the atmospheric channel, J. Opt. Fiber Commun. Res., pp.345–396, 2005.

[18] S. Schwartz, and Y. Yeh, "On the distribution function and moments of power sums with lognormal components, Bell Syst. Tech. J., vol. 61, no. 7, pp.1441–1462, 1982.
[19] D.A. Luong, T.C. Thang, and A.T. Pham, "Effect of avalanche photodiode and thermal noises on the performance of binary phase shift keyingsubcarrier-intensity modulation/free-space optical systems over turbulence channels," IET Commun., vol.7, no.8, pp.738–744, May 2013.
[20] M. Uysal, J.T. Li, and M. Yu, "Error rate performance analysis of coded free-space optical links over gamma-gamma atmospheric turbulence channels," IEEE Trans. Wireless Commun., vol.5, no.6, pp.1229–1233, June 2006.
[21] S.A. Ahmadi, and H. Yanikomeroglu, "On the Approximation of the PDF of the Sum of Independent Generalized-K RVs by Another Generalized-K PDF with Applications to Distributed Antenna Systems," Proc. WCNC, pp.1–6, Sydney, Australia, Apr. 2010.
[22] S. Xuegui, N. Mingbo, and J. Cheng, "Error Rate of Subcarrier Intensity Modulations for Wireless Optical Communications," IEEE Commun. Lett., vol.16, no.4, pp.540–543, Apr. 2012.

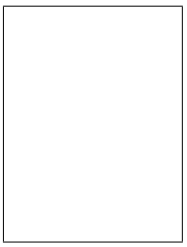

Vuong V. Mai received the B.E. degree from Posts and Telecommunications Institute of Technology, Vietnam in 2012. He is currently working toward a M.E. degree in Computer Network Systems at the University of Aizu, Japan. Mai's study in Japan is funded by a Japanese government scholarship (MonbuKagaku-sho). His current research focuses on cross-layer design and performance analysis of free-space optics (FSO) and Visible Light Communication (VLC). Mai is student member of IEEE.

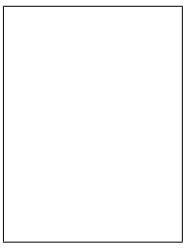

Anh T. PHAM received the B.E. and M.E. degrees, both in Electronics Engineering from the Hanoi University of Technology, Vietnam in 1997 and 2000, respectively, and the Ph.D. degree in Information and Mathematical Sciences from Saitama University, Japan in 2005. From 1998 to 2002, he was with the NTT Corp. in Vietnam. Since April 2005, he has been on the faculty at the University of Aizu, where he is currently a senior associate professor at the Computer Communications Laboratory, the School of Computer Science and Engineering. Dr. Pham also holds an adjunct professor position at Vietnam National University/University of Engineering and Technology. Dr. Pham's research interests are in the broad areas of communication theory and networking with a particular emphasis on modeling, design and performance evaluation of wired/wireless communication systems and networks. He received Japanese government scholarship (MonbuKagaku-sho) for Ph.D. study. He also received Vietnamese government scholarship for undergraduate study. Dr. Pham is senior member of IEEE. He is also member of IEICE and OSA.